24 April 2026

Density-Corrected Density Functional Theory for Solids

Youngsam Kim[1], Suhwan Song[1], Mihira Sogal[2], Kieron Burke[2,3], Eunji Sim[1]

1. Department of Chemistry, Yonsei University
2. Department of Chemistry, University of California
3. Department of Physics and Astronomy, University of California

Abstract

Density-corrected density functional theory (DC-DFT) considers whether self-consistent densities yield optimal energetics in Kohn-Sham calculations. With considerable success in molecular calculations, we here apply DC-DFT to solid-state calculations with Hartree-Fock (HF) densities. We resolve a known anomaly: that dispersion corrections can worsen results as one climbs Jacob's ladder. This is illustrated for simple covalent solids, such as Si. The relative energetics of phases of ice are also much improved with HF densities, as is CO absorption on NaCl, while graphite interlayer binding is insensitive to its density.

Density-Corrected Density Functional Theory for Solids

Youngsam Kim,[1] Suhwan Song,[1, †] Mihira Sogal,[2] Kieron Burke,[2, 3] and Eunji Sim[1, *]
[1] *Department of Chemistry, Yonsei University, 50 Yonsei-ro, Seodaemun-gu, Seoul 03722, Korea*
[2] *Department of Chemistry, University of California, Irvine, CA 92697, USA*
[3] *Department of Physics and Astronomy, University of California, Irvine, CA 92697, USA*

Density-corrected density functional theory (DC-DFT) considers whether self-consistent densities yield optimal energetics in Kohn-Sham calculations. With considerable success in molecular calculations, we here apply DC-DFT to solid-state calculations with Hartree-Fock (HF) densities. We resolve a known anomaly: that dispersion corrections can worsen results as one climbs Jacob's ladder. This is illustrated for simple covalent solids, such as Si. The relative energetics of phases of ice are also much improved with HF densities, as is CO absorption on NaCl, while graphite interlayer binding is insensitive to its density.

With the advent of high-throughput materials searches[1, 2] and machine-learned interatomic potentials[3–6], density functional theory (DFT), long a cornerstone of electronic structure theory[7], has become even more central to modern condensed-matter physics[8, 9] and materials science[10]. The predictive power of such calculations is commonly attributed to the accuracy of approximate exchange–correlation (XC) functionals,[11] implicitly assuming that the self-consistent electron density obtained from a given functional is sufficiently accurate. Well-known deficiencies include self-interaction and strong-correlation errors,[12–15] motivating extensive efforts to develop improved approximations along Jacob's ladder.[16–18]

However, not all failures of Kohn–Sham calculations can be attributed solely to the XC functional. The total energy error can be decomposed into functional and density-driven contributions, the latter arising from inaccuracies in the self-consistent density. This perspective underlies density-corrected DFT (DC-DFT),[19] which has been extensively studied in molecular systems. While most systems exhibit small density-driven errors (DDEs), those that do not can be substantially improved by evaluating functionals on alternative densities, and a wide range of chemical properties have been shown to be density-sensitive.[20–27] While this framework is well established in molecular systems, its implications for condensed-phase calculations remain less explored.

In pioneering work on surfaces, Patra *et al.*[28] applied PBE+U densities to the CO/Pt(111) puzzle[29], suggesting that density-driven self-interaction errors can dominate adsorption energetics and site preferences. Related studies have reported similar effects in molecule–surface systems[30, 31], transition-metal oxides[32], simulations of water[33], and aqueous radicals[34]. However, for condensed-phase systems, existing studies remain limited to specific cases, and a general understanding of DDEs across diverse bonding environments is still lacking. In particular, their role in the inconsistencies observed in standard solid-state calculations has not been systematically established. One manifestation of this problem is a long-standing paradox in solid-state DFT: dispersion interactions are known to be significant[35, 36], yet adding them to semilocal functionals does not lead to consistent improvement in accuracy.

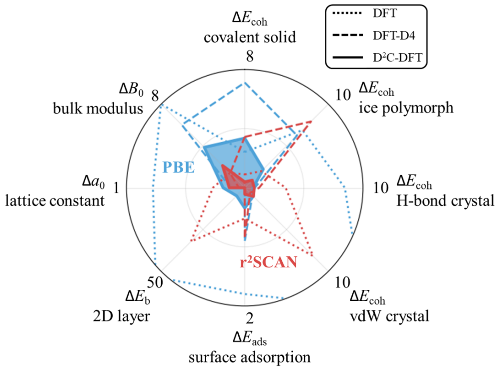

Figure 1. Comparison of pure DFT, dispersion-corrected DFT (DFT-D4), and density- and dispersion-corrected DFT (D^{2}C-DFT) across main-group non-metallic solids properties, grouped by bonding character. Errors are normalized to characteristic reference scales. Cohesive and adsorption energies ($\Delta E_{\rm coh}$, $\Delta E_{\rm ads}$) are reported in kcal/mol, graphite binding energies ($\Delta E_{\rm b}$) in meV/atom, and structural properties (lattice constants and bulk moduli) in %. Dispersion corrections produce nonuniform changes in accuracy across systems, an inconsistency that is resolved with the use of the HF density.

Figure 1 provides a representative overview of this trend across main-group non-metallic solids. A clear pattern emerges: the effect of dispersion corrections varies widely across systems, with no consistent improvement in agreement with reference data. This pattern cannot be explained by dispersion interactions alone and instead points to a more general source of error in condensed-phase DFT.

Here we show that this inconsistency correlates with the density sensitivity, whose magnitude varies with bonding character and can be significant even in systems traditionally regarded as well described by semilocal functionals. When density sensitivities are significant, the total energy can already be biased at the level of the self-consistent density, such that additional contributions, including dispersion, may amplify existing errors rather than improve agreement. By contrast, evaluating functionals on the HF density in these systems reduces these inconsistencies and restores physically consistent energetic trends. These results establish density sensitivity as a central factor governing the accuracy of DFT in condensed-phase systems.

Next, we briefly outline the theoretical framework underlying DDEs. For a given external potential $v(\mathbf{r})$, the total energy error arising from a self-consistent Kohn–Sham DFT[37] calculation can be decomposed as

$$\Delta E = \tilde{E}[\tilde{n}] - E[n] = (\tilde{E}_{\text{XC}}[n] - E_{\text{XC}}[n]) + (\tilde{E}[\tilde{n}] - \tilde{E}[n]), \tag{1}$$

where the first term is the functional error and the second is the DDE. The functional error reflects the intrinsic limitation of the approximate XC functional even when evaluated on the exact density, whereas the DDE arises from inaccuracies in the self-consistent density.

This separation underlies density-corrected DFT (DC-DFT), in which evaluating the functional on an alternative density can reduce energetic errors without modifying the functional when DDEs are significant.[38–41] In practice, for molecular calculations, a simple and widely used approach is to evaluate the XC functional on the HF density, which can yield improved energies for systems with large DDEs.[42, 43] However, in some problems, HF densities reduce errors by more than the DDE[44–47], so the success of HF-DFT[48, 49] remains to be understood.

A key diagnostic for identifying regimes with significant DDEs is the density sensitivity,[50] defined as

$$\tilde{S} = \left| \tilde{E}[n^{\text{HF}}] - \tilde{E}[n^{\text{LDA}}] \right|. \tag{2}$$

Large values of $\tilde{S}$ indicate that the approximate functional is highly sensitive to the density, such that errors in the self-consistent density can lead to large changes in the total energy, which signals a substantial DDE. Conversely, when $\tilde{S}$ is small, the energy is relatively insensitive to the density, and DDEs are expected to be small.

Inaccuracies in the self-consistent density can therefore lead to significant biases in the total energy and give rise to inconsistent energetic predictions. A prominent manifestation of this effect is that dispersion corrections may fail to improve agreement with reference energetics when evaluated on an inaccurate density and can even worsen it.

By contrast, when evaluated on the HF density, particularly in density-sensitive cases, these inconsistencies are largely removed, and dispersion corrections restore physically consistent energetics. This motivates the density- and dispersion-corrected DFT (D^{2}C-DFT) framework,[52, 53] in which dispersion corrections are evaluated on the HF density, while their parameters are determined so as to avoid contamination from DDEs. Recent progress in KS inversion for solids[54] further underscores the importance of the electron density itself in determining electronic properties, including band gaps.

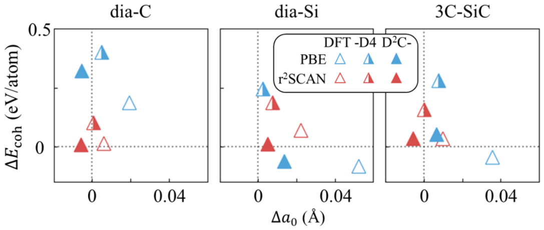

Figure 2. Effects of density and dispersion corrections in prototypical covalent solids. Errors in cohesive energy (ΔE_{coh}) and lattice constant (Δa_0) relative to reference values[51] are shown. The impact of dispersion corrections varies markedly with the underlying density, suggesting that energetic accuracy is governed by DDEs, as evidenced by the large density sensitivities (Table S3), even in covalent solids.

Before presenting the results, we briefly summarize the computational framework. We focus on representative semilocal generalized gradient approximation (GGA) and meta-GGA functionals, PBE[55] and r^{2}SCAN[56], evaluated in three forms: self-consistent DFT, dispersion-corrected DFT (DFT-D4), and D^{2}C-DFT. Dispersion interactions are treated using the D4 method.[57, 58] All calculations are well converged with respect to basis set, computational settings, and dispersion parameters; further details and validation are provided in the Supplemental Material[59], including Fig. S1, Tables S1–S2, and Refs.[60–64] therein.

We find that energetic predictions in DFT for main-group non-metallic solids are sensitive to the choice of density; and that the extent of this sensitivity varies across bonding regimes. As summarized in Fig. 1, dispersion corrections produce no consistent improvement in accuracy, indicating the presence of an additional source of error. This behavior is captured by the density sensitivity, suggesting contributions from DDEs.

Covalent solids— We first examine prototypical covalent solids: diamond C (dia-C), Si (dia-Si), and zincblende SiC (3C-SiC), where DDEs are commonly assumed to be negligible. To quantify energetic accuracy, we consider the cohesive energy,

$$E_{\text{coh}} = E_{\text{gas}} - E_{\text{crys}}, \tag{3}$$

where E_{crys} and E_{gas} are the crystal and isolated constituent energies, respectively, expressed per atom (or per molecule for molecular crystals).

Dispersion corrections are known to improve lattice constants but often worsen cohesive energies.[65, 66] Figure 2 shows this trend for representative covalent solids. This long-standing inconsistency arises in density-sensitive regimes, as additional attractive dispersion contributions amplify pre-existing energetic biases.

This apparent trade-off is not specific to DFT-D4 (see PBE+MBD@rsSCS and r^{2}SCAN+rVV10 in Fig. S2). Consistently, D^{2}C-DFT improves energetic predictions and alleviates the trade-off between lattice constants and cohesive energies.

Table I. Mean error (ME) and mean absolute error (MAE) in cohesive energies for the ICE7 and X23 datasets in kcal/mol. Experimental reference values are from Refs.[67] and [68]. The X23 dataset is divided into hydrogen-bond (H-bond), mixed (Mix), and van der Waals (vdW) subsets (number of systems in parentheses). The lowest MAE in each category is shown in bold. Density-corrected approaches improve accuracy in density-sensitive systems (*e.g.*, hydrogen-bonded) while maintaining comparable performance in density-insensitive cases.

			PBE			r^2SCAN		
		kcal/mol	D^2C-	-D4	DFT	D^2C-	-D4	DFT
ICE7		ME	0.3	1.3	-1.3	0.2	1.6	0.4
		MAE	**0.4**	1.3	1.4	**0.2**	1.6	0.4
X23	total (23)	ME	0.6	-0.4	-12.2	-0.6	0.1	-6.5
		MAE	**0.9**	**0.9**	12.2	1.0	**0.8**	6.5
	H-bond (8)	ME	0.1	0.2	-8.5	-0.2	1.1	-3.5
		MAE	**0.7**	0.9	8.5	**0.8**	1.2	3.5
	Mix (4)	ME	0.6	-0.1	-12.4	-0.8	0.0	-6.6
		MAE	0.8	**0.4**	12.4	0.8	**0.4**	6.6
	vdW (11)	ME	0.9	-1.0	-14.9	-0.9	-0.7	-8.7
		MAE	**1.1**	**1.1**	14.9	1.1	**0.7**	8.7

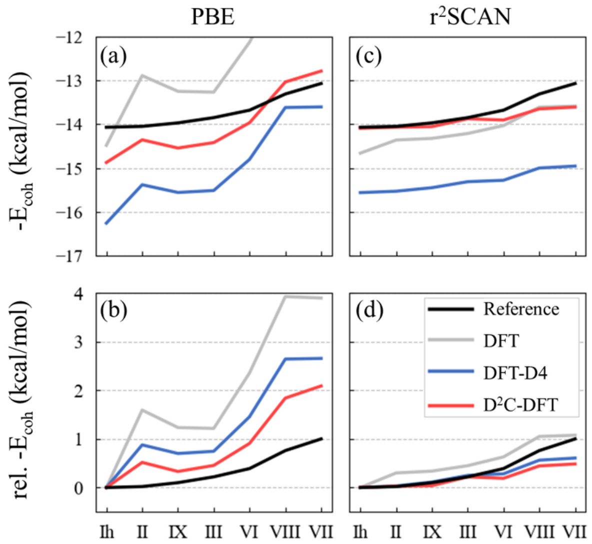

Figure 3. Cohesive energies of seven ice polymorphs (ICE7). Density correction restores agreement with experiment, which commensurate with the density sensitivities of hydrogen-bonded systems.

Table S3 shows that density sensitivities are irrelevant at the local density approximation (LDA) level but become significant for more accurate GGAs and meta-GGAs, in some cases comparable to or exceeding the total self-consistent DFT error. This could suggest that DDEs are not negligible even in prototypical covalent solids.

For the bulk modulus, density and dispersion corrections modify the values for both PBE and r^2SCAN, typically by about 2-4% (Table S4). Analysis of the equation-of-state curves[69, 70] in Table S5 further indicates that the dominant contribution to the overall discrepancy originates from cohesive energy errors, whereas higher-order volume terms such as the bulk modulus play only a minor role.

Molecular crystals— We next examine systems where DDEs are expected to be more pronounced, namely molecular crystals stabilized by hydrogen-bonds and dispersion interactions. The ICE7 dataset, comprising seven ice polymorphs with experimental references,[67] provide a stringent test, with cohesive energy differences of only ∼1 kcal/mol.[71, 72] As shown in Table I, dispersion corrections on self-consistent densities often overcorrect functional errors, leading to little improvement compared to pure DFT. D^2C- systematically reduces the mean absolute error to less than $\frac{1}{2}$ kcal/mol. As shown in Fig. 3, PBE underbinds while r^2SCAN slightly overbinds, and dispersion corrections improve relative ordering but often worsen absolute energies. D^2C-PBE substantially mitigates this inconsistency.

To extend beyond density-sensitive cases, we consider the X23 dataset[73–77] spanning hydrogen-bonded, mixed, and van der Waals crystals. Table I shows that the energetic predictions for hydrogen-bonded systems depend strongly on the choice of density, whereas dispersion-dominated systems are largely insensitive and already well described by dispersion-corrected DFT. Comparison with recent diffusion Monte Carlo results[78] in Table S6 confirms that these qualitative trends remain unchanged.

These trends can be understood in terms of the density sensitivity (Eq. 2). As shown in Fig. 4, systems separate according to this metric. Hydrogen-bonded crystals exhibit large values, suggesting substantial DDEs, whereas dispersion-dominated systems show minimal sensitivity, indicating weak density dependence. Importantly, the magnitude of density sensitivity is comparable to that of dispersion contributions, placing both effects on the same energetic scale.

Surface adsorption— We further test this framework in CO adsorption on NaCl(100)[79–81], where electrostatic interactions are expected to introduce intermediate DDEs. As shown in Fig. 5, dispersion-corrected DFT overestimates adsorption energies, whereas density correction systematically reduces overbinding. These results indicate that energetic predictions in surfaces depend sensitively on the choice of density.

Density-insensitive limit— Finally, graphite interlayer binding[82] represents a density-insensitive limit. The negligible density sensitivity suggests that DDEs are small and that binding is dominated by dispersion interactions (see Figs. S3-S4).

In summary, our results establish DDEs as the missing piece behind the nonuniform impact of dispersion corrections in condensed-phase DFT, as reflected in the density sensitivity and confirmed by the systematic improvement with D^2C-DFT. In density-sensitive regimes, dispersion

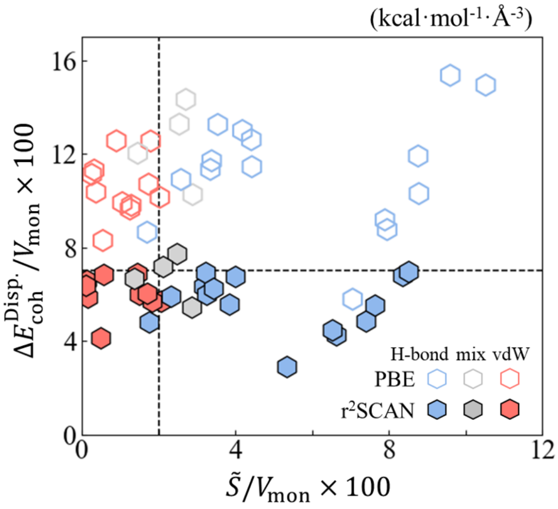

Figure 4. Density sensitivity $\tilde{S}$ versus dispersion contributions $\Delta E_{\mathrm{coh}}^{\mathrm{Disp.}}$ in molecular crystals (ICE7 and X23), with both quantities normalized by the monomer volume V_{mon}. Large density sensitivity signals regimes where DDEs dominate energetic errors, whereas small sensitivity indicates weak dependence on the density. The separation of systems according to bonding character is consistent across functionals, indicating that the dominant error regime is determined by bonding physics rather than by the choice of functional.

corrections can worsen energetic accuracy by reinforcing pre-existing errors, whereas D^{2}C-DFT can restore consistent accuracy. Density sensitivity thus serves as a practical indicator for identifying regimes where density correction is most beneficial.

Even in prototypical covalent solids, where density errors are commonly assumed negligible, density sensitivities can become comparable to the total self-consistent DFT error. Across molecular crystals, surface adsorption, and layered materials, this framework consistently explains when standard approximations succeed or fail, providing a unified description of binding across bulk, molecular, and interfacial environments.

Importantly, these results do not imply that HF densities are universally more accurate or should be adopted in all solid-state calculations. They would be inappropriate for metals, for example. But where appropriate in density-sensitive regimes, the D^{2}C-DFT framework consistently improves energetic predictions, suggesting that it mitigates density-driven contributions to the error. An alternative density worth exploring would be that of RPA[83, 84].

More broadly, our findings highlight the central role of the electron density in determining energetic accuracy and suggest that controlling DDEs will be essential for achieving consistent predictive performance in large-scale materials simulations. Challenges remain, including the scarcity of benchmark-quality reference data for extended systems and the cost of obtaining HF densities for large-scale calculations. Ongoing advances in high-level benchmarks and electronic-structure methods are expected to further clarify and extend the role of DC-DFT in condensed-phase systems.

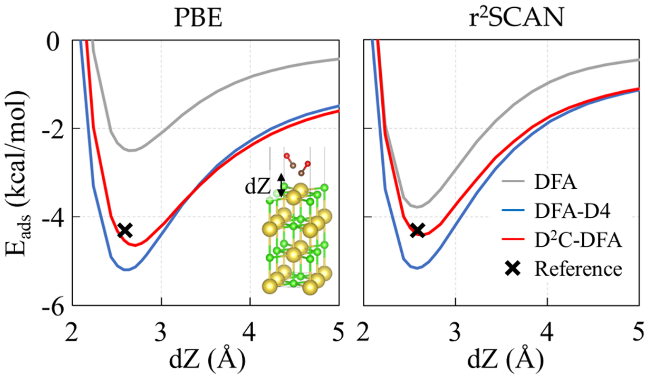

Figure 5. Potential energy surfaces for CO adsorption on NaCl(100). Dispersion corrections overbind adsorption energies, whereas D^{2}C-DFT restores agreement with experiment. The same framework consistently describes binding across bulk, molecular, and surface environments, highlighting the generality of DDEs in governing energetic accuracy.

Acknowledgments—We gratefully acknowledge support from the National Research Foundation of Korea (NRF-RS-2025-00554671), the Korea Environment Industry & Technology Institute (KEITI-RS-2023-00219144), and Samsung Electronics Co., Ltd. (DS Division, IO251223-14952-01). K.B. and M.S acknowledge support from NSF Grant No. DMR-2427903.

[†] Present address: Vertical AI2 Team, AI Center, Samsung Electronics, 130 Samsung-ro, Suwon, 16678, Korea
[*] esim@yonsei.ac.kr

[1] S. Curtarolo, G. L. Hart, M. B. Nardelli, N. Mingo, S. Sanvito, and O. Levy, The high-throughput highway to computational materials design, Nat. Mater **12**, 191 (2013).
[2] A. Nandy, C. Duan, M. G. Taylor, F. Liu, A. H. Steeves, and H. J. Kulik, Computational discovery of transition-metal complexes: From high-throughput screening to machine learning, Chem. Rev. **121**, 9927 (2021).
[3] I. Batatia, P. Benner, Y. Chiang, A. M. Elena, D. P. Kovács, J. Riebesell, X. R. Advincula, M. Asta, M. Avaylon, W. J. Baldwin, *et al.*, A foundation model for atomistic materials chemistry, J. Chem. Phys. **163** (2025).
[4] K. T. Schütt, H. E. Sauceda, P.-J. Kindermans, A. Tkatchenko, and K.-R. Müller, Schnet–a deep learning architecture for molecules and materials, J. Chem. Phys. **148** (2018).
[5] S. Batzner, A. Musaelian, L. Sun, M. Geiger, J. P. Mailoa, M. Kornbluth, N. Molinari, T. E. Smidt, and B. Kozinsky, E (3)-equivariant graph neural networks for data-efficient and accurate interatomic potentials, Nat. Commun. **13**, 2453 (2022).
[6] V. L. Deringer, M. A. Caro, and G. Csányi, Machine

learning interatomic potentials as emerging tools for materials science, Adv. Mater. **31**, 1902765 (2019).

[7] R. O. Jones, Density functional theory: Its origins, rise to prominence, and future, Rev. Mod. Phys. **87**, 897 (2015).

[8] P. J. Hasnip, K. Refson, M. I. Probert, J. R. Yates, S. J. Clark, and C. J. Pickard, Density functional theory in the solid state, Phil. Trans. R. Soc. A **372**, 20130270 (2014).

[9] J. P. Perdew, A. Ruzsinszky, G. I. Csonka, L. A. Constantin, and J. Sun, Workhorse semilocal density functional for condensed matter physics and quantum chemistry, Phys. Rev. Lett. **103**, 026403 (2009).

[10] J. Neugebauer and T. Hickel, Density functional theory in materials science, WIREs Comput. Mol. Sci. **3**, 438 (2013).

[11] N. Mardirossian and M. Head-Gordon, Thirty years of density functional theory in computational chemistry: an overview and extensive assessment of 200 density functionals, Mol. Phys. **115**, 2315 (2017).

[12] O. A. Vydrov, G. E. Scuseria, J. P. Perdew, A. Ruzsinszky, and G. I. Csonka, Scaling down the perdew-zunger self-interaction correction in many-electron regions, J. Chem. Phys. **124** (2006).

[13] P. Mori-Sánchez, A. J. Cohen, and W. Yang, Many-electron self-interaction error in approximate density functionals, J. Chem. Phys. **125** (2006).

[14] H. J. Kulik, M. Cococcioni, D. A. Scherlis, and N. Marzari, Density functional theory in transition-metal chemistry: A self-consistent hubbard u approach, Phys. Rev. Lett. **97**, 103001 (2006).

[15] A. J. Cohen, P. Mori-Sánchez, and W. Yang, Challenges for density functional theory, Chem. Rev. **112**, 289 (2012).

[16] N. Mardirossian and M. Head-Gordon, ωb97m-v: A combinatorially optimized, range-separated hybrid, meta-gga density functional with vv10 nonlocal correlation, J. Chem. Phys **144** (2016).

[17] S. Bi, S. Wang, I. Y. Zhang, and X. Xu, Improving xyg3-type doubly hybrid approximation using self-interaction corrected scan density and orbitals via the pz-sic framework: The xdh@ scan (sic) approach, J. Chem. Phys. **159** (2023).

[18] A. D. Becke, G. Santra, and J. M. Martin, A double-hybrid density functional based on good local physics with outstanding performance on the gmtkn55 database, J. Chem. Phys. **158** (2023).

[19] M.-C. Kim, E. Sim, and K. Burke, Understanding and reducing errors in density functional calculations, Phys. Rev. Lett. **111**, 073003 (2013).

[20] M.-C. Kim, E. Sim, and K. Burke, Ions in solution: Density corrected density functional theory (dc-dft), J. Chem. Phys. **140** (2014).

[21] E. Sim, M.-C. Kim, and K. Burke, Dissociation curves of diatomic molecules: A dc-dft study, in *AIP Conf. Proc.*, Vol. 1702 (AIP Publishing, 2015).

[22] M.-C. Kim, H. Park, S. Son, E. Sim, and K. Burke, Improved dft potential energy surfaces via improved densities, J. Phys. Chem. Lett. **6**, 3802 (2015).

[23] S. Song, M.-C. Kim, E. Sim, A. Benali, O. Heinonen, and K. Burke, Benchmarks and reliable dft results for spin gaps of small ligand fe (ii) complexes, J. Chem. Theory Comput. **14**, 2304 (2018).

[24] Y. Kim, S. Song, E. Sim, and K. Burke, Halogen and chalcogen binding dominated by density-driven errors, J. Phys. Chem. Lett. **10**, 295 (2018).

[25] S. Nam, E. Cho, E. Sim, and K. Burke, Explaining and fixing dft failures for torsional barriers, J. Phys. Chem. Lett. **12**, 2796 (2021).

[26] H. Yu, S. Song, S. Nam, K. Burke, and E. Sim, Density-corrected density functional theory for open shells: How to deal with spin contamination, J. Phys. Chem. Lett. **14**, 9230 (2023).

[27] Y. Kim, M. Sim, M. Lee, S. Kim, S. Song, K. Burke, and E. Sim, Extending density-corrected density functional theory to large molecular systems, J. Phys. Chem. Lett. **16**, 939 (2025).

[28] A. Patra, H. Peng, J. Sun, and J. P. Perdew, Rethinking co adsorption on transition-metal surfaces: Effect of density-driven self-interaction errors, Phys. Rev. B **100**, 035442 (2019).

[29] P. J. Feibelman, B. Hammer, J. K. Nørskov, F. Wagner, M. Scheffler, R. Stumpf, R. Watwe, and J. Dumesic, The co/pt (111) puzzle, J. Phys. Chem. B **105**, 4018 (2001).

[30] B. X. Shi and T. Berkelbach, Practical and improved density functionals for computational catalysis on metal surfaces, arXiv:2602.14962 (2026).

[31] A. Sachin and V. Voora, Resolving density errors enables accurate description of molecule–surface interactions for ionic materials, chemrxiv (2025).

[32] H. R. Gopidi, R. Zhang, Y. Wang, A. Patra, J. Sun, A. Ruzsinszky, J. P. Perdew, and P. Canepa, Reducing self-interaction error in transition-metal oxides with different exact-exchange fractions for energy and density, Phys. Rev. B **113**, 165115 (2026).

[33] S. Dasgupta, E. Lambros, J. P. Perdew, and F. Paesani, Elevating density functional theory to chemical accuracy for water simulations through a density-corrected many-body formalism, Nat. Commun. **12**, 6359 (2021).

[34] F. Belleflamme and J. Hutter, Radicals in aqueous solution: assessment of density-corrected scan functional, Phys. Chem. Chem. Phys. **25**, 20817 (2023).

[35] J. Klimeš and A. Michaelides, Perspective: Advances and challenges in treating van der waals dispersion forces in density functional theory, J. Chem. Phys. **137** (2012).

[36] J. Hermann, R. A. DiStasio Jr, and A. Tkatchenko, First-principles models for van der waals interactions in molecules and materials: Concepts, theory, and applications, Chem. Rev. **117**, 4714 (2017).

[37] W. Kohn and L. J. Sham, Self-consistent equations including exchange and correlation effects, Phys. Rev. **140**, A1133 (1965).

[38] A. Wasserman, J. Nafziger, K. Jiang, M.-C. Kim, E. Sim, and K. Burke, The importance of being inconsistent, Annu. Rev. Phys. Chem. **68**, 555 (2017).

[39] S. Vuckovic, S. Song, J. Kozlowski, E. Sim, and K. Burke, Density functional analysis: The theory of density-corrected dft, J. Chem. Theory Comput. **15**, 6636 (2019).

[40] S. Song, S. Vuckovic, E. Sim, and K. Burke, Density-corrected dft explained: Questions and answers, J. Chem. Theory Comput. **18**, 817 (2022).

[41] S. Nam, S. Song, E. Sim, and K. Burke, Measuring density-driven errors using kohn–sham inversion, J. Chem. Theory Comput. **16**, 5014 (2020).

[42] M.-C. Kim, E. Sim, and K. Burke, Communication: Avoiding unbound anions in density functional calculations, J. Chem. Phys. **134** (2011).

[43] E. Sim, S. Song, S. Vuckovic, and K. Burke, Improving results by improving densities: Density-corrected density functional theory, J. Am. Chem. Soc. **144**, 6625 (2022).

[44] A. D. Kaplan, C. Shahi, P. Bhetwal, R. K. Sah, and J. P. Perdew, Understanding density-driven errors for reaction barrier heights, J. Chem. Theory Comput. **19**, 532 (2023).

[45] B. Kanungo, A. D. Kaplan, C. Shahi, V. Gavini, and J. P. Perdew, Unconventional error cancellation explains the success of hartree–fock density functional theory for barrier heights, J. Phys. Chem. Lett. **15**, 323 (2024).

[46] A. D. Kaplan, C. Shahi, R. K. Sah, P. Bhetwal, B. Kanungo, V. Gavini, and J. P. Perdew, How does hf-dft achieve chemical accuracy for water clusters?, J. Chem. Theory Comput. **20**, 5517 (2024).

[47] N. Pangeni, C. Shahi, J. P. Perdew, V. Subramanian, B. Kanungo, V. Gavini, and A. Ruzsinszky, Hartree–fock density functional theory works through error cancellation for the interaction energies of halogen and chalcogen bonded complexes, J. Chem. Phys. **164** (2026).

[48] P. M. Gill, B. G. Johnson, J. A. Pople, and M. J. Frisch, An investigation of the performance of a hybrid of hartree-fock and density functional theory, Int. J. Quantum Chem. **44**, 319 (1992).

[49] B. G. Janesko and G. E. Scuseria, Hartree–fock orbitals significantly improve the reaction barrier heights predicted by semilocal density functionals, J. Chem. Phys. **128** (2008).

[50] E. Sim, S. Song, and K. Burke, Quantifying density errors in dft, J. Phys. Chem. Lett. **9**, 6385 (2018).

[51] L. Schimka, J. Harl, and G. Kresse, Improved hybrid functional for solids: The hsesol functional, J. Chem. Phys. **134** (2011).

[52] S. Song, S. Vuckovic, Y. Kim, H. Yu, E. Sim, and K. Burke, Extending density functional theory with near chemical accuracy beyond pure water, Nat. Commun. **14**, 799 (2023).

[53] M. Lee, B. Kim, M. Sim, M. Sogal, Y. Kim, H. Yu, K. Burke, and E. Sim, Correcting dispersion corrections with density-corrected dft, J. Chem. Theory Comput. **20**, 7155 (2024).

[54] V. Ravindran, N. I. Gidopoulos, and S. J. Clark, Local exchange-correlation potentials by density inversion in solids, Phys. Rev. B **112**, 085208 (2025).

[55] J. P. Perdew, K. Burke, and M. Ernzerhof, Generalized gradient approximation made simple, Phys. Rev. Lett. **77**, 3865 (1996).

[56] J. W. Furness, A. D. Kaplan, J. Ning, J. P. Perdew, and J. Sun, Accurate and numerically efficient r2scan meta-generalized gradient approximation, J. Phys. Chem. Lett. **11**, 8208 (2020).

[57] E. Caldeweyher, J.-M. Mewes, S. Ehlert, and S. Grimme, Extension and evaluation of the d4 london-dispersion model for periodic systems, Phys. Chem. Chem. Phys. **22**, 8499 (2020).

[58] S. Ehlert, U. Huniar, J. Ning, J. W. Furness, J. Sun, A. D. Kaplan, J. P. Perdew, and J. G. Brandenburg, r2scan-d4: Dispersion corrected meta-generalized gradient approximation for general chemical applications, J. Chem. Phys **154** (2021).

[59] See the Supplemental Material at [URL will be inserted by publisher] for additional details and data, and references therein.

[60] V. Blum, R. Gehrke, F. Hanke, P. Havu, V. Havu, X. Ren, K. Reuter, and M. Scheffler, Ab initio molecular simulations with numeric atom-centered orbitals, Comput. Phys. Commun. **180**, 2175 (2009).

[61] I. Y. Zhang, X. Ren, P. Rinke, V. Blum, and M. Scheffler, Numeric atom-centered-orbital basis sets with valence-correlation consistency from h to ar, New J. Phys. **15**, 123033 (2013).

[62] O. A. Loboda, G. A. Dolgonos, and A. D. Boese, Towards hybrid density functional calculations of molecular crystals via fragment-based methods, J. Chem. Phys. **149** (2018).

[63] Q. Sun, X. Zhang, S. Banerjee, P. Bao, M. Barbry, N. S. Blunt, N. A. Bogdanov, G. H. Booth, J. Chen, Z.-H. Cui, *et al.*, Recent developments in the pyscf program package, J. Chem. Phys. **153** (2020).

[64] G. Kresse and J. Furthmüller, Efficient iterative schemes for ab initio total-energy calculations using a plane-wave basis set, Phys. Rev. B **54**, 11169 (1996).

[65] G.-X. Zhang, A. Tkatchenko, J. Paier, H. Appel, and M. Scheffler, Van der waals interactions in ionic and semiconductor solids, Phys. Rev. Lett. **107**, 245501 (2011).

[66] W. Al-Saidi, V. K. Voora, and K. D. Jordan, An assessment of the vdw-ts method for extended systems, J. Chem. Theory Comput. **8**, 1503 (2012).

[67] J. G. Brandenburg, T. Maas, and S. Grimme, Benchmarking dft and semiempirical methods on structures and lattice energies for ten ice polymorphs, J. Chem. Phys. **142** (2015).

[68] G. A. Dolgonos, J. Hoja, and A. D. Boese, Revised values for the x23 benchmark set of molecular crystals, Phys. Chem. Chem. Phys. **21**, 24333 (2019).

[69] F. Birch, Finite elastic strain of cubic crystals, Phys. Rev. **71**, 809 (1947).

[70] K. Lejaeghere, V. Van Speybroeck, G. Van Oost, and S. Cottenier, Error estimates for solid-state density-functional theory predictions: an overview by means of the ground-state elemental crystals, Crit. Rev. Solid State Mater. Sci. **39**, 1 (2014).

[71] F. Della Pia, A. Zen, D. Alfè, and A. Michaelides, Dmc-ice13: Ambient and high pressure polymorphs of ice from diffusion monte carlo and density functional theory, J. Chem. Phys. **157** (2022).

[72] S. Grimme, A. Hansen, S. Ehlert, and J.-M. Mewes, r2scan-3c: A "swiss army knife" composite electronic-structure method, J. Chem. Phys. **154** (2021).

[73] A. M. Reilly and A. Tkatchenko, Understanding the role of vibrations, exact exchange, and many-body van der waals interactions in the cohesive properties of molecular crystals, J. Chem. Phys. **139** (2013).

[74] A. J. Price, A. Otero-de-la Roza, and E. R. Johnson, Xdm-corrected hybrid dft with numerical atomic orbitals predicts molecular crystal lattice energies with unprecedented accuracy, Chem. Sci. **14**, 1252 (2023).

[75] J. Klimeš, Lattice energies of molecular solids from the random phase approximation with singles corrections, J. Chem. Phys. **145** (2016).

[76] Y. H. Liang, H.-Z. Ye, and T. C. Berkelbach, Can spin-component scaled mp2 achieve kj/mol accuracy for cohesive energies of molecular crystals?, J. Phys. Chem. Lett. **14**, 10435 (2023).

[77] K. Syty, G. Czekalo, K. N. Pham, and M. Modrzejewski, Multi-level coupled-cluster description of crystal lattice energies, J. Chem. Theory Comput. (2025).

[78] F. Della Pia, A. Zen, D. Alfè, and A. Michaelides, How accurate are simulations and experiments for the lattice energies of molecular crystals?, Phys. Rev. Lett. **133**, 046401 (2024).

[79] J. Heidberg, E. Kampshoff, and M. Suhren, Correlation field, structure, and phase transition in the monolayer co adsorbed on nacl (100) as revealed from polarization fourier-transform infrared spectroscopy, J. Chem. Phys. **95**, 9408 (1991).

[80] G. Ewing, A model system for the study of structure and dynamics of molecules on surfaces: Co on nacl (100), Int. Rev. Phys. Chem. **10**, 391 (1991).

[81] J. Vogt and B. Vogt, The structure of carbon monoxide adsorbed on the nacl (100) surface—a combined leed and dft-d/vdw-df study, J. Chem. Phys. **141** (2014).

[82] L. Spanu, S. Sorella, and G. Galli, Nature and strength of interlayer binding in graphite, Phys. Rev. Lett. **103**, 196401 (2009).

[83] E. Trushin, S. Fauser, A. Mölkner, J. Erhard, and A. Görling, Accurate correlation potentials from the self-consistent random phase approximation, Phys. Rev. Lett. **134**, 016402 (2025).

[84] C. Shahi and J. P. Perdew, Comment on “accurate correlation potentials from the self-consistent random phase approximation”, Phys. Rev. Lett. **135**, 019601 (2025).